π- and σ-Diazo Radical Cations: Electronic and Molecular Structure of a Chemical Chameleon

Thomas Bally,*,† **Claudio Carra,**† **Stephan Matzinger,**† **Leo Truttmann,**† **Fabian Gerson,***,‡ **Reto Schmidlin,**‡ **Matthew S. Platz,***,§ **and Atnaf Admasu**§
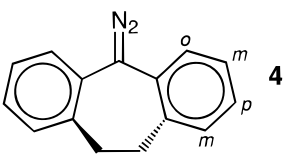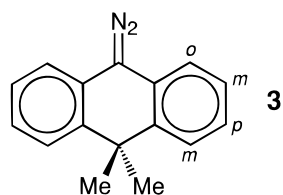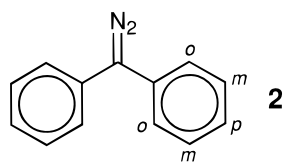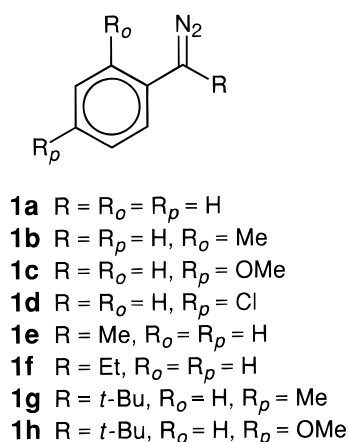
Contribution from the Institut de Chimie Physique, Université de Fribourg, Pérolles, CH-1700 Fribourg, Switzerland, Institut für Physikalische Chemie der Universität Basel, Klingelbergstrasse 80, CH-4056 Basel, Switzerland, and Department of Chemistry, The Ohio State University, Columbus, Ohio 43210

Received February 2, 1999

Abstract: Diphenyldiazomethane (**2**) and its $^{15}N_2$, ^{13}C, and D_{10} isotopomers, as well as the $C(Me)_2$ and CH_2-CH_2 bridged derivatives, 9-diazo-9,10-dihydro-10,10-dimethylanthracene (**3**) and 5-diazo-10,11-dihydro-5*H*-dibenzo[*a,d*]cycloheptene (**4**), are ionized by electrolytic and chemical oxidation in fluid solution and by γ-irradiation in Freon matrices. Depending on the experimental conditions of these reactions, two distinct species which correspond to π- and σ-radical states of the diazo radical cations are observed by optical and ESR spectroscopy. They drastically differ in their color, hyperfine pattern, and photostability. Theoretical calculations demonstrate that the experimentally found energetic proximity of the two states is not an intrinsic property of the diaryldiazo radical cations, but it must be due to some unidentified solvent (and/or counterion) effects acting to preferentially stabilize the σ-states by about 1 eV.

1. Introduction

In 1987, Ishiguro et al.[1] demonstrated for the first time that the radical cations of diazo compounds can be observed if they are carefully prepared by electrochemical oxidation in dichloromethane at low temperature. Thereby, the electronic structure of the radical cations of phenyldiazomethane (**1a**) and several derivatives (**1b**−**1h**) was found to depend sensitively on the substituents attached to the diazo and phenyl groups.[1,2] Whereas the ESR spectra of the radical cations **1a**•+−**1f**•+ exhibited large ^{14}N-coupling constants ($|a_N|$ = 1 to 2 mT) and their broad lines did not reveal the presence of ^1H-hyperfine splittings ($|a_H|$ < 0.2 mT), the radical cations **1g**•+ and **1h**•+, with a *tert*-butyl substituent on the diazo group, gave rise to well-resolved hyperfine patterns due to small and middle-sized $|a_N|$ and $|a_H|$ values (<0.5 mT).

1a R = R_o = R_p = H
1b R = R_p = H, R_o = Me
1c R = R_o = H, R_p = OMe
1d R = R_o = H, R_p = Cl
1e R = Me, R_o = R_p = H
1f R = Et, R_o = R_p = H
1g R = *t*-Bu, R_o = H, R_p = Me
1h R = *t*-Bu, R_o = H, R_p = OMe

The authors[1,2] interpreted these results in terms of two different "electromers" of the diazo radical cations,[3] one in which the unpaired electron occupies an allylic π-MO in a linear diazo group ("π-radical cation" with small and middle-sized $|a_H|$ and $|a_N|$ values) and another one with a bent diazo group and the unpaired electron residing in the N lone-pair MOs ("σ-radical cation" with large $|a_N|$ and unobservably small $|a_H|$ values). In the absence of aryl groups, the "bent" σ-states of diazo radical cations lie much higher than the "linear" π-states, but, according to Ishiguro et al.,[1,2] interaction of the diazo π-HOMO with the symmetric component of the HOMO of an adjacent phenyl group might entail a sufficiently great splitting of these two levels to cause the out-of-phase combination to be raised above the level of the σ-LUMO at the bent geometry. Therefore, such a combination of π-MOs would become the singly occupied MO (SOMO) at the expense of the (now higher lying) nonbonding allylic π-MO, as shown in Figure 1.[1,2] The presence of the bulky *tert*-butyl substituent should force the diazo group to be twisted out of the phenyl plane (or vice versa), thus inhibiting the conjugative interaction which is required to favor the bent σ-state.

In addition, the radical cation of diphenyldiazomethane (**2**) was also studied and classified as a σ-radical cation by virtue of its ESR spectrum with $|a_N|$ = 1.72 and 1.01 mT.[1,2] In another contribution, the results of oxidation experiments on derivatives of **2** by cyclic voltammetry at low temperature were reported.[4] Thereby, *two* reduction waves were found for various diphenyldiazomethanes, whereas the *tert*-butyl derivatives **1g** and **1h** showed only one. The two waves were assigned to the reduction of the initially formed π-radical cation and its σ-counterpart to

(1) Ishiguro, K.; Sawaki, Y.; Izuoka, A.; Sugawara, T.; Iwamura, H. *J. Am. Chem. Soc.* **1987**, *109*, 2530.

(2) Ishiguro, K.; Ikeda, M.; Sawaki, Y. *J. Org. Chem.* **1992**, *57*, 3057.

(3) The term "electromers" was originally introduced by Fry to denote electronic isomers in an early theory of chemical bonding (Fry, H. S. E. *Physik. Chem.* **1911**, *76*, 398). It was recently reintroduced to the literature to denote ground-state radical ion structures having the same atomic connectivity but a distinctly different distribution of spin and charge (Fiedler, A.; Schröder, D.; Shaik, S.; Schwarz, H. *J. Am. Chem. Soc.* **1994**, *116*, 10734. Shaik, S.; Danovitch, D.; Fiedler, A.; Schröder, D.; Schwarz, H. *Helv. Chim. Acta* **1995**, *78*, 1393).

(4) Ishiguro, K.; Ikeda, M.; Sawaki, Y. *Chem. Lett.* **1991**, 511.

† Université de Fribourg.
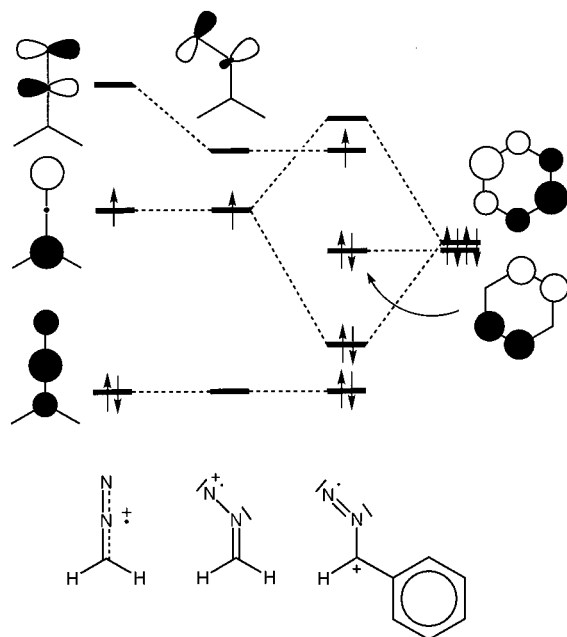‡ Universität Basel.
§ The Ohio State University.

Figure 1. MO scheme depicting the interaction of the most relevant MOs of diazomethane with the HOMO of benzene (following Ishiguro et al.[1,2]). It shows that the allylic π-SOMO of the diazomethane radical cation is raised *above* the σ-LUMO by this interaction (note that two different valence structures are drawn for the σ-radical cations of diazomethane and its phenyl derivative; this choice will be explained in section 5).

which the former was converted. By changing the temperature and the sweep rate, an activation energy of ca. 13 kcal/mol was determined for such a conversion in the radical cation of the dimesityl derivative.[4]

In 1987, Kato et al.[5] followed the radiolytic oxidation of **1a** and **2** at 77 K by ESR and optical spectroscopy. Radiolysis of **2** in a butyl chloride glass gave rise to a strong absorption at 650 nm that was assigned to **2**•+ and could be readily bleached by visible light to yield conjecturally the radical cation of diphenylcarbene. A few years ago, we picked up this thread by studying **2**•+ and its decomposition product in various Freon matrices.[6] Thereby, we made the striking observation that the color of the γ-irradiated samples, as well as their ESR spectra, depended on the type of Freon: In CFCl₃, CF₃CCl₃, and CF₂-ClCFCl₂, photostable pale pink samples were obtained, whereas radiolysis in CF₂BrCF₂Br or its mixture with CFCl₃ yielded blue samples of the type observed previously in butyl chloride.[5] Photolysis at $\lambda > 540$ nm caused the disappearance of the 650 nm band and led to ESR spectra expected for the radical cation of diphenylcarbene.[6]

In the present paper, we describe the optical and ESR spectra of **2**•+ and several isotopomers (¹³C, ¹⁵N₂, D₁₀) in more detail. Included are also the radical cations of the bridged derivatives **3** and **4**. The studies were carried out both on fluid solutions and in Freon matrices, and they corroborate the observation that the electronic structure of these radical cations critically depends not only on their chemical composition[1,2,4] but also on the experimental conditions under which such species are generated.[6] We also report the results of various quantum chemical calculations on the above and simpler model compounds, which show that the comparative stabilities of the π- and the σ-radical

cations of diphenyldiazo compounds are *not* an intrinsic property of these molecules.

2. Methods

2.1. Syntheses. Diaryldiazomethanes were prepared from the corresponding diaryl ketones which were converted either to hydrazones or to toluenesulfonyl (tosyl) hydrazones. Hydrazones were oxidized to diazo compounds with HgO (procedure A),[7] whereas tosyl hydrazones were converted to salts which were pyrolyzed under vacuum to give diazo compounds distilling out of the pyrolysis flask (procedure B).[8,9] Diaryldiazomethanes **2**,[7] **3**,[10] and **4**[11] are known and were synthesized using procedure A. The isotopomers [D₁₀]**2**[12] and [¹³C]**2** (labeled at the diazo carbon atom)[13] are also known and were prepared from benzophenone-D₁₀ and benzophenone-¹³C (Merck Isotopes), respectively, via procedure B.

The synthesis of [¹⁵N₂]**2** started from ¹⁵N-labeled hydrazine sulfate (Merck) which was converted into the correspondingly labeled toluenesulfone hydrazide. The tosyl hydrazone obtained after reaction with benzophenone was converted to the requisite diazo compound by procedure B.[8,9]

2.2. Sample Preparation. Solutions of the neutral diazo compounds ($\sim 10^{-2}$ M) were prepared in CFCl₃ (F-11) and CF₂BrCF₂Br (F-114B2) for ESR spectroscopy or in a 1:1 mixture of the two Freons for optical measurements.[14,15] These solutions were placed into quartz tubes (ESR work) or special optical cuvettes,[16] where they were exposed to 0.5 Mrad of ⁶⁰Co γ-radiation at 77 K. Anodic and chemical oxidations were effected at about 190 K in carefully dried dichloromethane.

The electrolysis was carried out in a cylindrical cell comprising a helical gold anode with a platinum wire along its axis as a counter-electrode.[17] Tetra-*n*-butylammonium tetrafluoroborate (0.1 M) served as the supporting salt, and a few drops of 2,6-dimethylpyridine (2,6-lutidine) were added as a proton scavenger. The chemical oxidation of **3** and **4** was performed with tris(4-bromophenyl)ammoniumyl hexachloroantimonate ("magic blue"), while **2** had to be treated with the more powerful oxidant, the corresponding salt of tris(2,4-dibromophenyl)-ammoniumyl ("magic green").[18] Unfortunately, the stronger reagent also oxidized the lutidine, which made it more difficult to prevent acid-catalyzed side reactions in this case.

2.3. Instrumental. Electronic absorption (EA) was measured on a Perkin Elmer Lambda-19 spectrometer (200−2000 nm). ESR spectra were taken on a Varian E9 instrument or a Bruker ESP-300 system, with the latter also serving for the ENDOR and TRIPLE-resonance studies.

2.4. Quantum Chemical Calculations. The geometries of all species were optimized by the B3LYP density functional method as implemented in the Gaussian 94 package of programs.[19,20] For the geometry optimizations, the standard 6-31G* basis set was employed, whereas the EPR III basis set of Barone[21] served for single-point calculations of the Fermi contact terms that can be converted into hyperfine-coupling constants.

(5) Kato, N.; Miyazaki, T.; Fueki, K.; Kobayashi, N.; Ishiguro, K.; Sawaki, Y. *J. Chem. Soc., Perkin Trans. 2* **1987**, 881.

(6) Bally, T.; Matzinger, S.; Truttman, L.; Platz, M. S.; Admasu, A.; Gerson, F.; Arnold, A.; Schmidlin, R. *J. Am. Chem. Soc.* **1993**, *115*, 7007.

(7) Smith, L. I.; Howard, K. L. *Organic Syntheses*; Wiley & Sons: New York, 1955; Collect. Vol. III, p 351.

(8) Closs, G. L.; Moss, R. A. *J. Am. Chem. Soc.* **1964**, *86*, 4042.

(9) Sugiyama, M. H.; Celebi, S.; Platz, M. S. *J. Am. Chem. Soc.* **1992**, *114*, 966.

(10) Wright, B. B.; Platz, M. S. *J. Am. Chem. Soc.* **1984**, *106*, 4175.

(11) Moritani, I.; Murahashi, S.-I.; Ashitaka, H.; Kimura, K.; Tsubomura, H. *Tetrahedron Lett.* **1966**, 373. *J. Am. Chem. Soc.* **1968**, *90*, 5918.

(12) Despres, A.; Lejeune, V.; Migirdicyan, E.; Admasu, A.; Platz, M. S.; Berthier, G.; Parisel, O.; Flament, J. P.; Beraldi, I.; Momicchioli, F. *J. Phys. Chem.* **1993**, *97*, 13358.

(13) Brandon, R. W.; Closs, G. L.; Davoust, C. E.; Hutchinson, C. A.; Kohler, B. E.; Silbey, R. *J. Chem. Phys.* **1965**, *43*, 2006.

(14) Sandorfy, C. *Can. J. Spectrosc.* **1965**, *85*, 10.

(15) Grimison, A.; Simpson, G. A. *J. Phys. Chem.* **1968**, *72*, 1776.

(16) Bally, T. In *Radical Ionic Systems*; Lund, A., Shiotani, M., Eds.; Kluwer: Dordrecht, 1991; pp 3−54.

(17) Ohya-Nishiguchi, H. *Bull. Chem. Soc. Jpn.* **1979**, *52*, 2064.

(18) Schmidt, W.; Steckhan, E. *Chem. Ber.* **1980**, *113*, 577.

(19) Frisch, M. J.; Trucks, G. W.; Schlegel, H. B.; Gill, P. M. W.; Johnson, B. G.; Robb, M. A.; Cheeseman, J. R.; Keith, T.; Petersson, G. A.; Montgomery, J. A.; Raghavachari, K.; Al-Laham, M. A.; Zakrzewski, V. G.; Ortiz, J. V.; Foresman, J. B.; Cioslowski, J.; Stefanov, B. B.; Nanayakkara, A.; Challacombe, M.; Peng, C. Y.; Ayala, P. Y.; Chen, W.;

π- *and* σ-*Diazo Radical Cations*

J. Am. Chem. Soc., Vol. 121, No. 30, 1999 7013

For the radical cations of parent diazomethane and its phenyl derivative, single-point calculations were carried out on B3LYP equilibrium geometries by the RCCSD(T) method[22] with Dunning's correlation-consistent polarized double- or triple-ζ basis sets (cc-pVDZ, cc-pVTZ),[23] employing the MOLPRO program.[24] For the excited states of **2•+**, we resorted to the CASSCF/CASPT2 procedure[25] with the MOLCAS program,[26] using the [C]3s2p1d/[H]2s ANO DZ basis set of Pierloot et al.[27] (a description of the active spaces is given in the footnotes to Table 1). In both cases, we had to apply level shifts to eliminate intruder states,[28] ensuring in each case that the energies of those states that were well described without level shifts remained roughly constant. Molecular orbitals were plotted with the MOPLOT program[29] which gives a schematic representation of the MOs' nodal structures in a ZDO-type approximation.[30]

3. Results and Discussion

3.1. Optical Spectra. Figure 2 shows the optical spectra of **2•+**, **3•+**, and **4•+** in the CFCl₃/CF₂BrCF₂Br mixture at 77 K (solid lines), as well as those of the carbene radical cations obtained by their photolysis at λ > 540 nm (dashed lines). The similarities within the two sets of spectra are obvious in that all primary radical cations show two strong bands peaking around 650 and 350 nm (the weak features at 400−450 nm are due to an unidentified secondary product), whereas the carbene radical cations obtained by photodeazotation are distinguished by a strong absorption peaking at 390−400 nm and flanked by a shoulder or a separate weak band at 440−510 nm.[6] As will be explained below, we assign the primary spectra to the π-radical states of the diazo cations.

After much trial and error, CASSCF/CASPT2 calculations on **2•+** led us to a satisfactory description of all excited states of interest, which is represented in Table 1. To aid the interpretation of these results, one may consider the MO diagram in Figure 3 which depicts how the relevant MOs of **2** arise through interaction of the three diazo orbitals on the right with the appropriate linear combinations of the benzene FMOs on the left.[31]

Thus, the strong band peaking at 660 nm in **2•+** can be unambiguously assigned to the 27a → 24b (SOMO) transition. It is characterized by a substantial amount of charge transfer

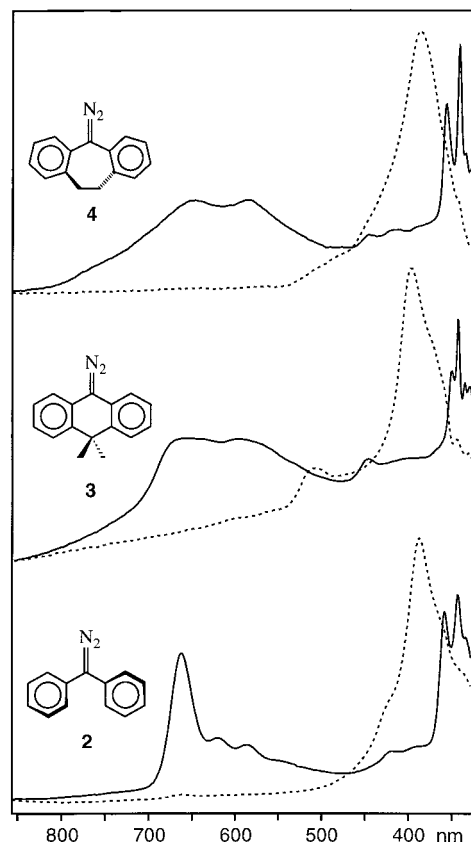**Figure 2.** Optical spectra of **2**, **3**, and **4** ionized by γ-irradiation in a 1:1 mixture of CFCl₃ and CF₂BrCF₂Br at 77 K (solid lines) and the corresponding carbene radical cations (dashed lines) obtained by subsequent photolytic deazotation (λ > 540 nm).

from the phenyl rings to the diazo group, which contributes to the strong transition moment. CASPT2 predicts it to be preceded by an excitation from the SOMO to the in-plane N₂ π*-MO, which may be responsible for the weak, broad shoulder on the low-energy side of the 660 nm band. Following this transition, we found two transitions with very small oscillator strengths; they involve more excitations from the three benzene MOs (26a, 27a, and 23b) into the SOMO and are likely to contribute to the high-energy tail of the main band system in the visible.

The next two transitions into the 4²B and the 5²B states are interesting because they are essentially composed of the same two excitations, 22b → SOMO and SOMO → LUMO. However, the 1²B → 4²B transition carries almost no oscillator strength, whereas the other one is apparently responsible for the intense UV band in the spectrum of **2•+**. An analysis shows that both excitations are associated with sizable transition moments which nearly cancel in the negative combination but reinforce each other in the positive one.[32] This situation is reminiscent of that in radical cations of polyenes[33,34] or in those of naphthalene derivatives[35] where addition and cancellation of transition moments for pairs of excitations also leads to similar pairs of weak and strong bands in the optical spectra.

Finally, CASPT2 predicts a number of rather weak transitions above 4 eV (below 300 nm) which involve mostly excitations from the three doubly occupied benzene π-MOs that do not interact with the diazo group into the in-plane N₂ π*-MO

Wong, M. W.; Andres, J. L.; Repogle, E. S.; Gomperts, R.; Martin, R. L.; Fox, D. J.; Binkley, J. S.; DeFrees, D. J.; Baker, J.; Stewart, J. P.; Head-Gordon, M.; Gonzalez, C.; Pople, J. A. Gaussian 94, Rev. B1 and D4; Gaussian, Inc.: Pittsburgh, PA, 1995.

(20) For a description of the DFT methods implemented in the Gaussian program, see: Johnson, B. G.; Gill, P. M. W.; Pople, J. A. *J. Chem. Phys.* **1993**, *98*, 5612.

(21) Barone, V. *Theor. Chim. Acta* **1995**, *91*, 113.

(22) Coupled cluster method with single and double excitations, based on a spin-restricted HF zero-order wave function and supplemented by a noniterative estimation of the contributions of triple excitations. Knowles, P. J.; Hampel, C.; Werner, H.-J. *J. Chem. Phys.* **1993**, *99*, 5219.

(23) Woon, D. E.; Dunning, T. H., Jr. *J. Chem. Phys.* **1993**, *98*, 1358.

(24) Werner, J.-J.; Knowles, P. J.; Almlöf, J.; Amos, R. D.; Deegan, M. J. O.; Elbert, S. T.; Hampel, C.; Meyer, W.; Peterson, K.; Pitzer, R.; Stone, A. J.; Taylor, P. R.; Lindh, R.: MOLPRO, 96.1 (1996).

(25) Andersson, K.; Roos, B. O. In *Modern Electronic Structure Theory*; World Scientific Publ. Co.: Singapore, 1995; Vol. Part 1, Vol. 2; p 55.

(26) Andersson, K.; Blomberg, M. R. A.; Fülscher, M. P.; Kellö, V.; Lindh, R.; Malmqvist, P.-Å.; Noga, J.; Olson, J.; Roos, B. O.; Sadlej, A.; Siegbahn, P. E. M.; Urban, M.; Widmark, P.-O. MOLCAS, Versions 3 and 4; University of Lund: Sweden, 1994.

(27) Pierloot, K.; Dumez, B.; Widmark, P.-O.; Roos, B. O. *Theor. Chim. Acta* **1995**, *90*, 87.

(28) Roos, B. O.; Andersson, K.; Fülscher, M. P.; Serrano-Andrés, L.; Pierloot, K.; Merchán, M.; Molina, V. *J. Mol. Struct. (THEOCHEM)* **1996**, *388*, 257.

(29) Bally, T.; Albrecht, B.; Matzinger, S.; Sastry, M. G. MOPLOT, a program for displaying results of LCAO-MO calculations, available from Thomas.Bally@unifr.ch on request.

(30) Haselbach, E.; Schmelzer, A. *Helv. Chim. Acta* **1971**, *54*, 1299.

(31) The configurational description in the last column of Table 1 is given in terms of a CASSCF wave function including only the MOs depicted in Figure 3. This procedure is justified because, with the larger active spaces which are necessary to arrive at satisfactory CASPT2 wave functions and energies, big rotations among the MOs of the same symmetries lead to a loss of the transparency obtained at the (9,11)CASSCF level.

Table 1. Excited States of the Radical Cation of Diphenyldiazomethane (2[•+])

states	EAS eV	CASSCF[a] eV	CASPT2[b] eV	f^{d}	major configurations[c]	
1[2]B	(0)	(0)	(0)		91%	(24b)[1]
2[2]B	(~1.7)	3.06	1.98	0.004	83%	24b → 26b
1[2]A	1.9	2.01	2.09	0.249	64%	27a → 24b
					+9%	26b → 24b
2[2]A	(~2.3)	2.26	2.32	0.001	62%	26b → 24b
					+7%	27a → 24b
3[2]B	(~2.3)	3.29	2.32	0.010	74%	23b → 24b
4[2]B		3.61	2.60	2 × 10^{−4}	35%	24b → 25b
					−36%	22b → 24b
5[2]B	3.6	4.74	3.29	0.279	37%	24b → 25b
					+28%	22b → 24b
6[2]B[e]		4.42	4.15	>10[−4]	66%	23b → 26b
3[2]A		3.99	4.21	0.019	77%	27a → 26b[g]
4[2]A		4.46	4.43	0.003	62%	26a → 26b[g]
5[2]A		4.60	4.54	0.017	44%	26a → 26b[g]
					31%	27a → 26b[g]
6[2]A[f]		5.03	4.59	0.145	44%	27a → 26b[g]
					32%	26a → 26b[g]

[a] The active space comprises 9 electrons in the 11 MOs depicted in Figure 2, augmented by one doubly occupied a-MO (π-MO centered on the benzene rings) for the A-states, and two doubly occupied b-MOs (centered on the CN$_2$ moiety) for the B-states; averaging was carried out over 6 states of each symmetry. [b] Calculated with a level shift of 0.1 a.u. for the A-states and 0.2 a.u. for the B-states. [c] In a (9,11) CASSCF wave function. [d] Oscillator strength for electronic transition, based on the CASSCF wave function and the CASPT2 energy difference. [e] This state is poorly described at the (13,13)CASPT2 level used for the other B-states, energies and oscillator strength from (11,12)CASPT2. [f] This state is poorly described at the (11,12)CASPT2 level used for the A-states, energies and oscillator strength from (9,11)CASPT2. [g] See ref 36.

(26b).[36] However, in view of the fact that neutral absorptions block our view on the cations below 330 nm, we were satisfied with the finding that obviously no important state that might contribute to the spectra above 300 nm had been missed. Thus, we conclude that our assignment of the optical spectra obtained by ionization of diphenyldiazomethanes in CFCl$_3$/CF$_2$BrCF$_2$Br to the π-radical states of the diazo cations is in accordance with the calculations described above.

3.2. ESR Spectra. Diphenyldiazomethane (2). Figure 4 displays the ESR spectra of 2[•+], [15N$_2$]2[•+], and [13C]2[•+] observed upon electrolytic oxidation of the corresponding neutral compounds in dichloromethane at 183 K. In agreement with previously reported data,[1,2] the hyperfine pattern of 2[•+] (Figure 4, top) consists of two ^{14}N-triplets due to the coupling constants $|a_N| = 1.68 \pm 0.02$ and 1.01 ± 0.02 mT. The hyperfine splittings from the phenyl protons in 2[•+] are concealed by the line-width of ca. 0.4 mT; they must be less than 0.2 mT.

The two ^{15}N-doublets in the spectrum of [15N$_2$]2[•+] (Figure 4, center), with $|a_N| = 2.36 \pm 0.02$ and 1.42 ± 0.02 mT, exactly match the hyperfine pattern expected for the replacement of the

(32) The phases of the MOs can be chosen such that the directions of the transition moments are reverted. However, this alternative entails a change in the sign of the CI coefficients, so that the final result remains the same.

(33) Bally, T.; Nitsche, S.; Roth, K.; Haselbach, E. *J. Am. Chem. Soc.* **1984**, *106*, 3927.

(34) Fülscher, M. P.; Matzinger, S.; Bally, T. *Chem. Phys. Lett.* **1995**, *236*, 167.

(35) Bally, T.; Carra, C.; Fülscher, M. P.; Zhu, Z. *J. Chem. Soc., Perkin Trans. 2* **1998**, 1759.

(36) Excitations from doubly occupied into virtual MOs of radicals cannot be described correctly by single configurations, of which three must be combined into so-called configuration state functions. As a consequence, the contributions of the 26a → 26b and the 26a → 26b excitations add up to more than 100% in the final-state wave functions.
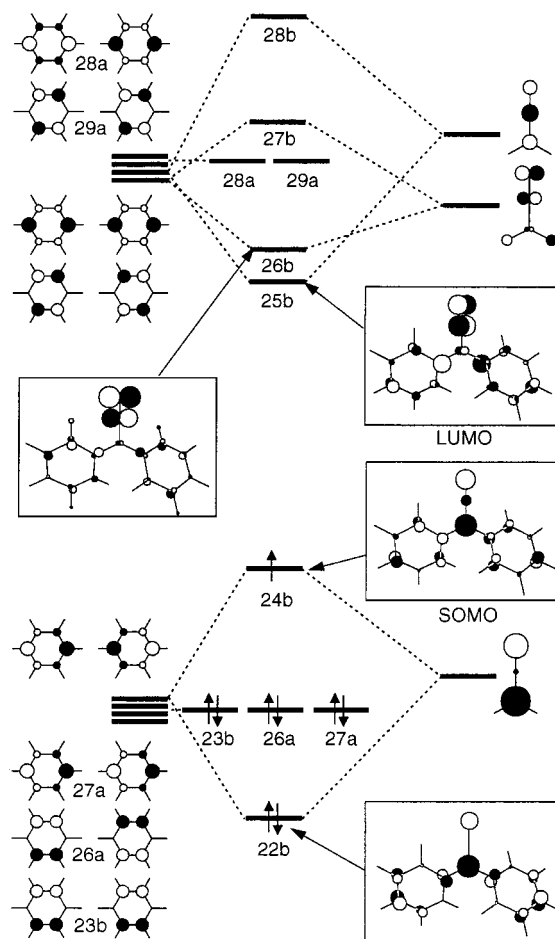

Figure 3. Graphical representation of the results of CASSCF/CASPT2 calculations on the electronic structure of the π-radical state of 2[•+].

two ^{14}N nuclei in 2[•+] by their ^{15}N isotopes. In the ESR spectrum of [13C]2[•+] (Figure 4, bottom), an additional doublet splitting relative to that of 2[•+] indicates a coupling constant, $|a_C| = 3.35 \pm 0.05$ mT, of the ^{13}C nucleus in the diazo carbon atom. The spectrum of [D$_{10}$]2[•+] (not reproduced here) closely resembles that of 2[•+], except for some narrowing of the ^{14}N-hyperfine components. Clearly, the spectra of 2[•+] and its isotopomers generated by electrolytic oxidation must be attributed to a σ-radical cation.

B3LYP/EPRIII calculations indicate that the larger $|a_N|$ value should be assigned to the ^{14}N nucleus in the central nitrogen atom (N$_c$) sharing the C−N bond, thus leaving the smaller one for the terminal atom (N$_t$). Actually, as formulated for 2[•+], [15N$_2$]-2[•+], and [13C]2[•+] in Figure 4 and for the σ-radical cations of diazo compounds throughout the paper, the bulk of the spin is expected to reside at the terminal atom, N$_t$. However, the spin population at this atom has a predominant "p-character" and, therefore, gives rise to a hyperfine interaction weaker than that at the central atom, N$_c$, which has a marked s-contribution (see also section 5). Such an s-contribution to the spin population at the diazo carbon atom must also be responsible for the observed large ^{13}C-coupling constant.

After a few minutes, the ESR spectrum of 2[•+] disappeared. Continued electrolysis gave rise to a secondary paramagnetic species which was identified by its highly resolved hyperfine pattern with the well-known radical cation of tetraphenylethene (5).[37]

(37) Lewis, I. C.; Singer, L. S. *J. Chem. Phys.* **1965**, *43*, 2712. Reymond, A.; Fraenkel, G. K. *J. Phys. Chem.* **1967**, *71*, 4570.
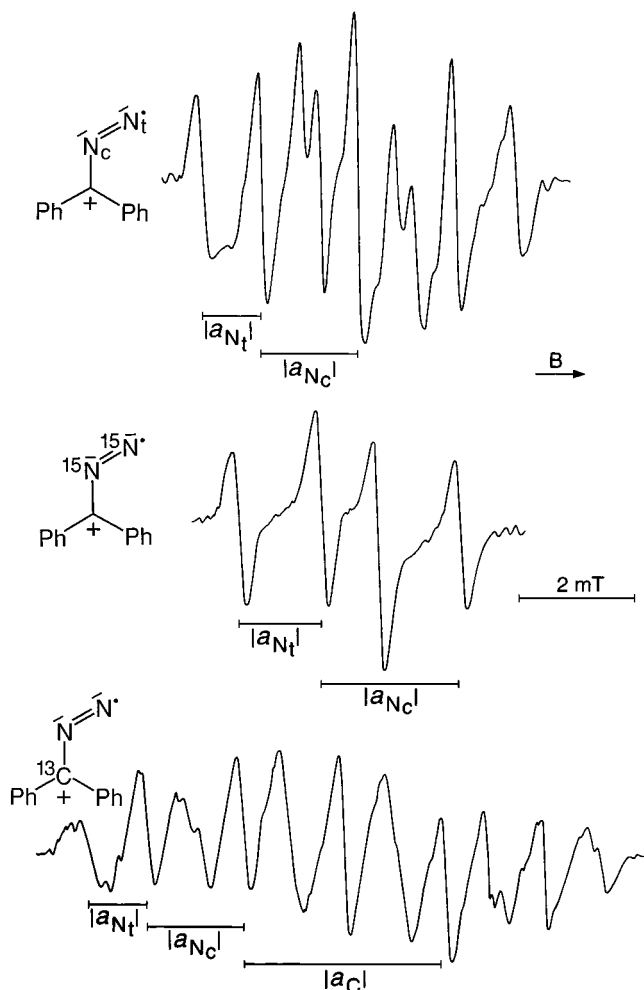
Figure 4. ESR spectra of the radical cations **2**[•+] (top), [[15]N$_2$]**2**[•+] (center), and [^{13}C]**2**[•+] (bottom) generated electrolytically in dichloromethane at 183 K, counterion BF$_4^-$.

Upon chemical oxidation of **2** with magic green in dichloromethane at 198 K, a completely different ESR spectrum, presented in Figure 5 (top) along with its computer simulation (center), was observed. The much narrower and richer hyperfine pattern obtained under these conditions is due to coupling constants $|a_N| = 0.44 \pm 0.01$ and 0.33 ± 0.01 mT, each for a single ^{14}N nucleus, and $|a_H| = 0.34 \pm 0.01$, 0.25 ± 0.01, and 0.096 ± 0.005 mT for two, four, and four protons, respectively. These values are comparable to the ones found by Ishiguro et al.[1,2] in the case of *tert*-butyl-substituted phenyldiazomethanes, **1g**[•+] and **1h**[•+], and assigned in terms of their linear π-state. Starting from [D$_{10}$]**2**, a ^{14}N-quintet spaced by 0.39 ± 0.02 mT was obtained (Figure 5, bottom). This spectrum of [D$_{10}$]**2**[•+] obviously arises from the two ^{14}N nuclei, with the difference in their $|a_N|$ values and the splittings by the phenyl deuterons being unresolved. With the aid of the calculations, the $|a_H|$ values of **2**[•+] are assigned, in the above sequence, to the protons in the para, ortho, and meta positions of the two phenyl groups. The same calculations predict almost equal $|a_N|$ values for the two ^{14}N nuclei of the linear diazo moiety, albeit with different signs (see below). The larger value is tentatively assigned to N$_t$.[38]

The π-radical cation **2**[•+] was too short-lived for the observation of its ENDOR spectrum. Raising the temperature led to a disappearance of the ESR spectrum of **2**[•+], without any signals

---

(38) A table containing all measured and calculated hyperfine-coupling constants is available in the Supporting Information.
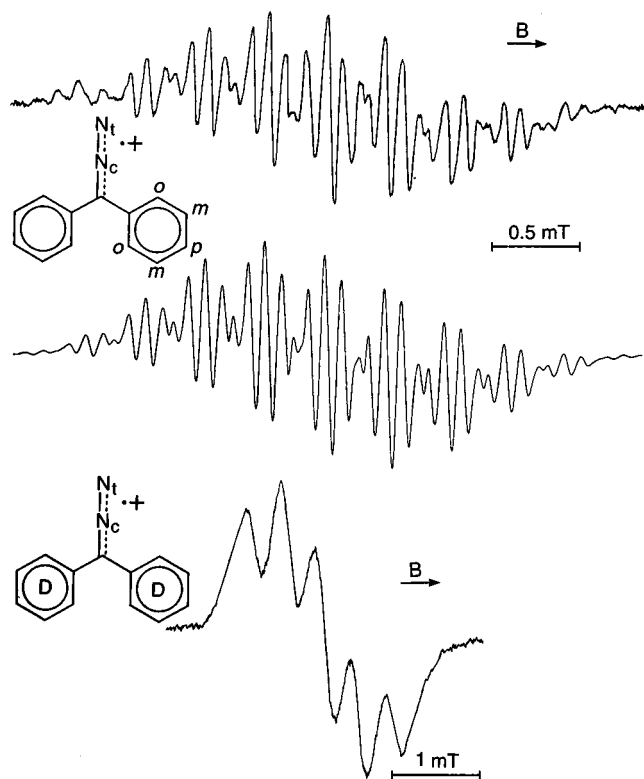

Figure 5. ESR spectra of the radical cation **2**[•+] (top) and [D$_{10}$]**2**[•+] (bottom) generated with magic green in dichloromethane at 198, counterion SbCl$_6^-$. Computer simulation (center) of the upper spectrum using the coupling constants given in the text, a Lorentzian line-shape, and a line-width of 0.06 mT. Note the different field-scale for the spectra of **2**[•+] and [D$_{10}$]**2**[•+].

due to a secondary species following. However, in some experiments, oxidation of **2** with magic green in dichloromethane yielded the persistent radical cation **5**[•+] instead of **2**[•+]. Under these conditions, not only the ESR spectrum of **5**[•+] but also the corresponding [1]H-ENDOR signals, which, in general, cannot be observed during the electrolysis, were likewise recorded.[39,40]

γ-Irradiation of **2** in a CFCl$_3$ matrix produced a sample of light pink color. The prominent feature of the corresponding ESR spectrum is a pronounced g anisotropy which makes it extend over 28 mT.[41] The two ^{14}N-coupling constants, associated with the three g components (2.042 ± 0.004, 2.001 ± 0.002, and 1.965 ± 0.005) are, respectively, $|a_N| = 3.6 \pm 0.3$, ~0, and 3.6 ± 0.4 mT for the larger value, and 2.0 ± 0.3, ~0, and 2.0 ± 0.4 mT for the smaller one. Averaging yields $|a_N| = 2.4 \pm 0.4$ and 1.3 ± 0.3 mT. Although these values greatly exceed the isotropic ^{14}N-coupling constants measured for **2**[•+] in fluid solution, they are (together with the color of the matrix) diagnostic of the σ-state of the radical cation. Similar statements hold true also for the ESR spectra of [[15]N$_2$]**2**[•+], [^{13}C]**2**[•+], and

---

(39) The coupling constants, $|a_H| = 0.292 \pm 0.02$, 0.206 ± 0.02, and 0.053 ± 0.01 mT, assigned to the four para, eight ortho, and eight meta protons, respectively, in the four phenyl substituents of **5**[•+], agree with the values reported in the literature.[37] General-TRIPLE-resonance experiments[40] indicated that the smallest $|a_H|$ value has a sign opposite to the two larger ones; the former is undoubtedly positive, while the latter have a negative sign.

(40) Kurreck, H.; Kirste, B.; Lubitz, W. *Electron Nuclear Double Resonance of Radicals in Solution*; VCH: New York, 1988; Chapter 2.

(41) The ESR spectrum of **2**[•+] in a CFCl$_3$ matrix was previously described.[5] However, these authors overlooked the extended lateral features, due to the g anisotropy, and considered only the central, relatively narrow signal. The ESR spectra of **2**[•+] and [^{13}C]**2**[•+] observed by us with Freon matrices are available in the Supporting Information.

[D$_{10}$]**2**$^{•+}$ in CFCl$_3$ matrices. Corresponding ENDOR signals could not be detected for either **2**$^{•+}$ or its isotopomers in CFCl$_3$.

In contrast, the deep blue color of the γ-irradiated CF$_2$BrCF$_2$-Br matrices containing **2**$^{•+}$, [^{13}C]**2**$^{•+}$, [^{15}N$_2$]**2**$^{•+}$, and [D$_{10}$]**2**$^{•+}$, as well as their ESR and ENDOR spectra, clearly characterized these species as π-radical cations, in accordance with the conclusions reached on the basis of the optical spectrum of **2**$^{•+}$ in the same matrix. The ESR spectra showed hardly any *g* anisotropy and consisted essentially of one signal extending over several mT. At low temperatures, such a signal was bare of hyperfine pattern, but, in the case of [^{13}C]**2**$^{•+}$, warming of the CF$_2$BrCF$_2$Br matrix to 140 K revealed a partially resolved splitting due to the coupling constant, $|a_C| = 1.2 \pm 0.1$ mT, of the ^{13}C isotope in the diazo carbon atom.

Although the corresponding ENDOR spectra of **2**$^{•+}$ and its isotopomers in CF$_2$BrCF$_2$Br were readily obtained, the low signal-to-noise ratio and residual hyperfine anisotropy[42] made them very difficult to analyze. Nevertheless, ^{14}N- and ^{1}H-coupling constants comparable to those observed upon oxidation of **2** with magic green were determined from pairs of signals in the frequency range 4−8 MHz, and separated by $2\nu_N = 2.1$ MHz, as well as from those in the range 8−21 MHz and centered at $\nu_H = 14.5$ MHz. Moreover, in the ENDOR spectrum of [^{13}C]**2**$^{•+}$, an additional pair of signals, centered at 15.8 MHz and separated by $2\nu_C = 7.3$ MHz, indicated a coupling constant $|a_C| = 1.13 \pm 0.05$ mT.

As emphasized in a previous paper[6] and shown in Figure 2 above, the diphenylcarbene radical cation was photolytically produced from the π-radical cations **2**$^{•+}$ and [^{13}C]**2**$^{•+}$ in CF$_2$BrCF$_2$Br matrices, but it was not formed starting from the σ-counterparts of these diazo precursors in CFCl$_3$ glasses.

9-Diazo-9,10-dihydro-10,10-dimethylanthracene (3). The well-resolved ESR spectrum of **3**$^{•+}$ generated electrolytically from **3** in dichloromethane was simulated in terms of ^{14}N- and ^{1}H-coupling constants, $|a_N| = 0.40 \pm 0.01$ (1N) and 0.32 $\pm$ 0.01 mT (1N) and $|a_H| = 0.32 \pm 0.01$ (2H), 0.24 $\pm$ 0.01 (2H), and 0.076 $\pm$ 0.005 mT (4H).[43] On the basis of the calculations, the $|a_H|$ values were assigned to the para, ortho, and meta protons in the two phenylene groups, respectively. The hyperfine splittings by the six protons of the two methyl substituents were too small to be resolved ($|a_H| < 0.02$ mT). Evidently, **3**$^{•+}$ must be classified as a π-radical cation, in contrast to **2**$^{•+}$ generated under exactly the same conditions.

The radical cation **3**$^{•+}$ also gradually decayed, and upon prolonged electrolysis, an ESR spectrum with a similar hyperfine pattern but a smaller extent (1.8 instead of 2.8 mT) appeared; it was readily attributed to the hitherto unknown radical cation of 10,10,10′,10′-tetramethyl-9,9′-bi-9*H*-anthracenylidene (**6**). The ^{1}H-coupling constants found for **6**$^{•+}$ are $|a_H| = 0.207 \pm 0.002, 0.157 \pm 0.002$, and 0.056 ± 0.001 mT for the four para, four ortho, and eight meta protons, respectively, in the four phenylene groups.[43] B3LYP/6-31G* optimization of **6**$^{•+}$ resulted in a dihedral angle of 69° between the two anthracenylidene moieties.

Chemical oxidation with magic blue in dichloromethane at 198 K produced either the π-radical cation **3**$^{•+}$ or the more persistent **6**$^{•+}$, whereby formation of the former was favored by addition of the proton scavenger, 2,6-lutidine. For **6**$^{•+}$, the corresponding ENDOR spectrum could now also be obtained, by which the three $|a_H|$ values given above were confirmed, and from which the smallest coupling constant, $|a_H| = 0.007 \pm 0.001$ mT, due to the twelve protons of the four methyl substituents in **6**$^{•+}$, was derived.[43] According to general-

6
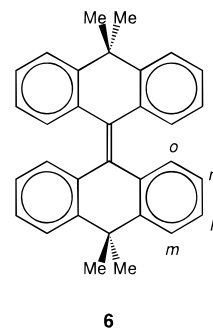
TRIPLE-resonance experiments,[40] the sign of 0.056 mT is opposite to that of the two larger values; theoretically, the former must be positive, and the latter negative. The coupling constant of the methyl protons is presumably positive.

γ-Irradiation of **3** in both CFCl$_3$ and CF$_2$BrCF$_2$Br matrices caused a deep-blue coloring of the samples. The pertinent ESR spectra consisted of a broad signal ∼4 mT wide; that observed with a CFCl$_3$ matrix exhibited partly resolved hyperfine splittings of 0.25−0.40 mT. Despite complications due to a poor signal-to-noise ratio and residual hyperfine anisotropy, the corresponding ENDOR spectra[42] pointed to ^{14}N- and ^{1}H-coupling constants comparable to those found for electrolytically and chemically generated **3**$^{•+}$ in fluid dichloromethane. Undoubtedly, the radical cation produced in either matrix has also a linear π-radical structure.

5-Diazo-10,11-dihydro-5*H*-dibenzo[*a,d*]cycloheptene (4). Electrolysis of **4** in dichloromethane at 183 K led to the ESR spectrum of **4**$^{•+}$ reproduced in Figure 6 (top). This spectrum is much like that of **2**$^{•+}$ taken under the same conditions, and the two large ^{14}N-coupling constants $|a_N| = 1.84 \pm 0.02$ and 1.02 $\pm$ 0.02 mT clearly classify **4**$^{•+}$ as a σ-radical cation. However, closer inspection of the spectrum reveals some lack of symmetry, as a consequence of the superposition by an additional hyperfine pattern of another paramagnetic species present in much lower concentration. This pattern strikingly differs from the main spectrum of the σ-radical cation by a higher *g* factor (difference ∼0.002), a smaller extension (4 vs 6 mT), and narrower lines (width 0.05 vs 0.25 mT).

A partly resolved ESR spectrum, in conformity with the characteristics of the species in question, was observed upon chemical oxidation of **4** with magic blue in dichloromethane (Figure 6, center). Its analysis, verified by computer simulation, made use of the ^{14}N- and ^{1}H-coupling constants determined from the corresponding ENDOR spectrum (Figure 6, bottom). The pertinent values are $|a_N| = 0.44$ and 0.38 mT and $|a_H| = 0.35, 0.26, 0.08, 0.47$, and 0.18 mT (exptl error: ± 0.01 mT); the coupling constants $|a_H|$ were assigned, in this sequence, to the two para, two ortho, and four meta protons in the two phenylene groups, and to the pairs of axial and equatorial methylene protons. The hyperfine data for the chemically generated **4**$^{•+}$ thus clearly point to a π-radical structure. It is appealing to suggest that electrolytic oxidation of **4** also produces a π-radical cation, albeit in much lower concentration than its σ-counterpart. A secondary paramagnetic species, the radical cation of 10,10′,11,11′-tetrahydro-bi-5*H*-dibenzo[*a,d*]cycloheptenylidene, which would be analogous to **5**$^{•+}$ and **6**$^{•+}$ in the case of **2** and **3**, respectively, seemed not to be formed from **4**.

The behavior of **4** upon γ-irradiation in Freon matrices matched that of **2** under the same conditions. Thus, the ESR spectrum of **4**$^{•+}$ in the pink-colored CFCl$_3$ matrices was

---

(42) Gerson, F. *Acc. Chem. Res.* **1994**, *27*, 63.

(43) The ESR spectrum of **3**$^{•+}$ and its simulation, as well as the ESR and ENDOR spectra of **6**$^{•+}$, are available in the Supporting Information.
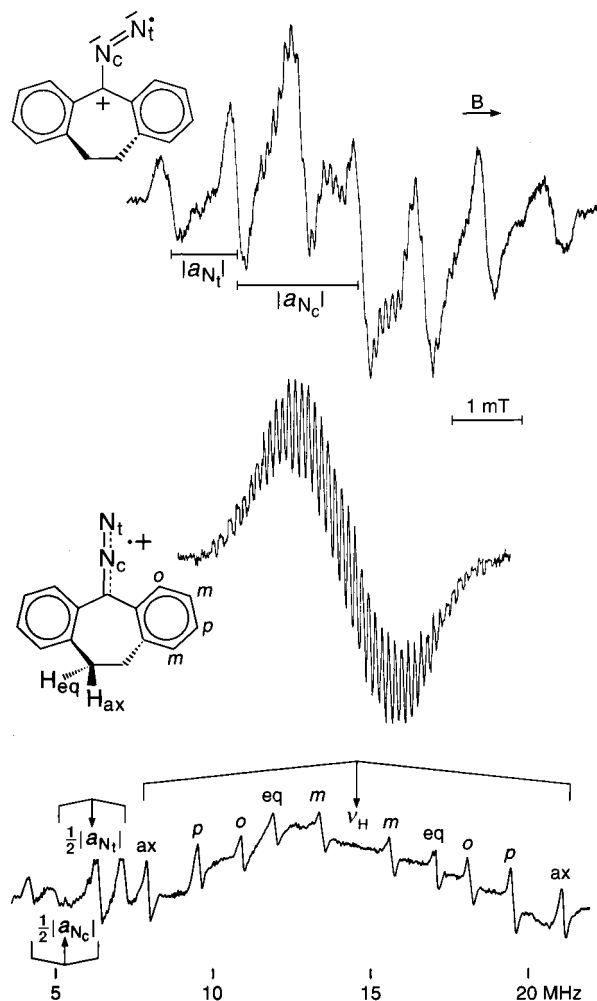
π- and σ-Diazo Radical Cations

J. Am. Chem. Soc., Vol. 121, No. 30, 1999   7017

Figure 7. ^{14}N-, ^{1}H-, and ^{13}C-coupling constants, in mT, for σ-**2**$^{•+}$ and π-**2**$^{•+}$. The H atoms are omitted for clarity (*: not observed). Assignment of the absolute values 0.44 and 0.33 to the two ^{14}N nuclei in π-**2**$^{•+}$ is uncertain.

be quite similar for the σ-radical cations, σ-**2**$^{•+}$ and σ-**4**$^{•+}$, on one hand, and for the π-radical cations, π-**2**$^{•+}$, π-**3**$^{•+}$, and π-**4**$^{•+}$, on the other hand. They are in agreement with the results of B3LYP/EPR-III calculations which provided not only the assignments (see above) but also the signs of the observed coupling constants.[44] Thus, a_N of both N_t (terminal) and N_c (central) in σ-**2**$^{•+}$ and σ-**4**$^{•+}$ must be *positive*. In the π-radical cations, a *positive* sign is required for a_N of N_t and a_H of the meta Hs, but a *negative* one for a_N of N_c and a_H of the para and ortho Hs. Finally, a_C of the diazo-C in either σ-**2**$^{•+}$ or π-**2**$^{•+}$, as well as a_H of the methylene Hs in π-**4**$^{•+}$, should be positive. The hyperfine data for σ-**2**$^{•+}$ and π-**2**$^{•+}$ are reproduced in Figure 7 as an illustration. The g factors are 2.0009 ± 0.0002 for the σ- and 2.0027 ± 0.0002 for the π-radical cations.

4. The Enigmatic Energetics of the Two States of 2$_•^+$

To support their hypothesis that the σ-radical states of aryldiazomethane radical cations are of similar stability as their π-counterparts, Ishiguro et al.[2] performed single-point UMP2/ STO-3G calculations at UHF/STO-3G geometries. According to these calculations, the energy difference between the linear π- and the less stable bent σ-radical state is reduced from 53.3 kcal/mol for the radical cation of parent diazomethane to 8.6 kcal/mol at the UHF level and to near zero for that of phenyldiazomethane, **1a**$^{•+}$, at the UMP2 level, a result which was in perfect accord with the experimental findings. We were able to confirm these numbers but noted an extreme degree of spin contamination in the UHF wave functions ($\langle S^2 \rangle$ is 2.68 and 2.34 for the π- and the σ-radical state, respectively, at the UHF/STO-3G geometries, instead of the correct value of 0.75 for doublets!), which shows that the above numbers are essentially meaningless.[45,46]

Indeed, exploratory B3LYP/6-31G* calculations indicated that the above assessment of the σ/π-energy gap in **1a**$^{•+}$ was completely off the mark. To put our own evaluations of this property onto a sound footing, we resorted to the stepwise validation procedure depicted in Figure 8. Calculations at a reliable reference level of theory (RCCSD(T)/cc-pVTZ) on the parent diazomethane radical cation led to a σ/π-gap of 66.0 kcal/ mol, which decreased to 64.8 kcal/mol on going to the smaller cc-pVDZ basis set. At the B3LYP/6-31G* level it was 61.6

Figure 6. ESR (top and center) and ENDOR (bottom) spectra of the radical cation **4**$^{•+}$ in dichloromethane; generated electrolytically (top) at 183 K, counterion BF$_4^-$, and with magic blue (center and bottom) at 198 K, counterion SbCl$_6^-$.

Table 2. Electronic Structure of the Radical Cations **2**$^{•+}$, **3**$^{•+}$, and **4**$^{•+}$ Generated under Various Conditions

solution	oxidation by	solvent (counterion)	**2**$^{•+}$	**3**$^{•+}$	**4**$^{•+}$
fluid	electrolysis	CH$_2$Cl$_2$ (BF$_4^-$)	σ	π	σ (π)
fluid	ammoniumyl^a	CH$_2$Cl$_2$ (SbCl$_6^-$)	π	π	π
matrix	γ-rays	CFCl$_3$^{b}	σ	π	σ
matrix	γ-rays	CF$_2$BrCF$_2$Br^b	π	π	π

^{a} Tris(4-bromophenyl)- or tris(2,4-dibromophenyl)ammoniumyl hexachloroantimonate (magic blue or magic green, respectively). ^{b} In Freon matrixes, the counterion is the radical anion of the Freon. However, it is is not in direct contact with the radical cation, and its influence can therefore be neglected.

diagnostic of a σ-radical cation. It likewise exhibited a pronounced g anisotropy which made it extend over nearly 30 mT and which prevented a corresponding ENDOR spectrum from being observed. On the other hand, with a CF$_2$BrCF$_2$Br matrix, a blue coloration occurred, and the ESR spectrum of **4**$^{•+}$ was only 5 mT wide. The pertinent ENDOR signals from protons and, in particular, those from the ^{14}N nuclei appeared at the frequencies expected for the coupling constants of a π-radical cation **4**$^{•+}$.

Summarizing the above results, Table 2 specifies the electronic structure, σ or π, of **2**$^{•+}$, **3**$^{•+}$, and **4**$^{•+}$, as derived from the ESR studies of these radical cations in fluid CH$_2$Cl$_2$ solutions upon electrolytic and chemical oxidation and in γ-irradiated CFCl$_3$ and CF$_2$BrCF$_2$Br matrixes. The hyperfine data prove to
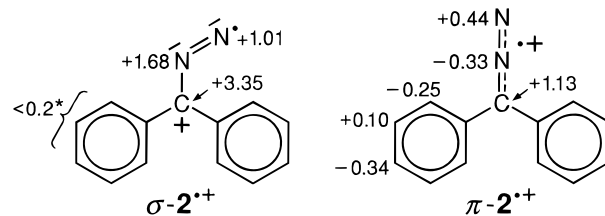
(44) All experimental and calculated hyperfine data characterizing the σ- and π-structures of **2**$^{•+}$ and **4**$^{•+}$, as well as the π-structure of **3**$^{•+}$, are compiled in the table which is contained in the Supporting Information.

(45) Bally, T.; Borden, W. T. In *Reviews in Computational Chemistry*; Lipkowitz, K. B., Boyd, D. B., Eds.; VCH-Wiley: New York, 1999; Vol. 13; p 1.

(46) Upon projection of the quartet components, the (P)UMP2/STO-3G σ/π-gap increases to nearly 80 kcal/mol! Such problems can be avoided by going to the spin-restricted MP2 method (RMP2). With the 6-31G* basis set, this method predicts a σ/π-gap of nearly 40 kcal/mol which also turns out to be significantly too high (see below). Thus, the MP2 method may be inherently inadequate for estimating the energy difference between the delocalized π-radical and the localized σ-radical state.
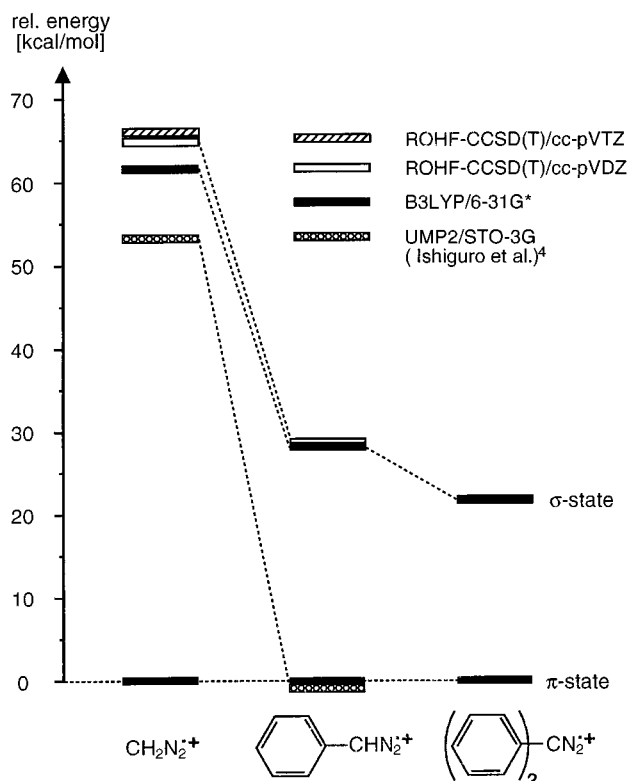
Figure 8. Calculated σ/π-gaps for the radical cations of parent diazomethane as well as for those of the phenyl (**1a**) and diphenyl derivative (**2**) by different methods.

Figure 9. Selected structural parameters of the π- and σ-radical states of the radical cations of diazomethane, **1a**, **2**, and **3**. Bond lengths in pm, angles in degrees. Full sets of Cartesian coordinates are available in the Supporting Information.

kcal/mol (augmenting the basis set to cc-pVTZ raised it to 63.6 kcal/mol), which reveals a tendency of B3LYP to slightly *underestimate* the σ/π-gap in diazomethane radical cations, especially with DZ basis sets.

In the phenyldiazomethane radical cation, **1a**[•+],[47] the σ/π-gap decreased to 28.8 kcal/mol by RCCSD(T)/cc-pVDZ. In this case, the corresponding B3LYP/ 6-31G* prediction (28.2 kcal/mol) agrees closely with that of the coupled cluster calculation but, as we have seen above, σ/π-gap of diazo radical cations calculated with DZ basis sets should be regarded as a lower boundary, and the actual value may well be a few kcal/mol higher.

For **2**[•+], coupled cluster calculations are no longer feasible because of its size and the lack of symmetry in the σ-radical state. However, the above validation procedure induces confidence in B3LYP/6-31G* as a predictor of the σ/π-gap in diazomethane radical cations. Due to the steric interaction of the facing ortho hydrogen atoms, **2**[•+] is no longer planar (see Figure 9). Consequently, the conjugative effect of the two phenyl rings on the σ/π-gap cannot simply be twice that of a single phenyl ring.

It was impossible to locate a minimum for the σ-radical state of **2**[•+], as it has no symmetry element to distinguish it from the π-state, to which it collapses invariably on unconstrained geometry optimization. Therefore, we had to turn to **3**[•+] where the presence of a symmetry plane prohibits the two states from mixing. Thereby, we found a σ-radical state, 18.4 kcal/mol above the π-state, but the C−N−N angle was opened from 120.2° in **1a**[•+] to 130.6° in **3**[•+], owing to the steric interaction

---

(47) Two conformations are possible for the bent σ-radical state. Both are minima of planar geometry on the B3LYP/ 6-31G* potential energy surface but, as the anti conformer turned out to be 5.2 kcal/mol more stable than its syn counterpart (where the N_2 group is bent towards the phenyl ring), the latter was disregarded in the subsequent calculations.
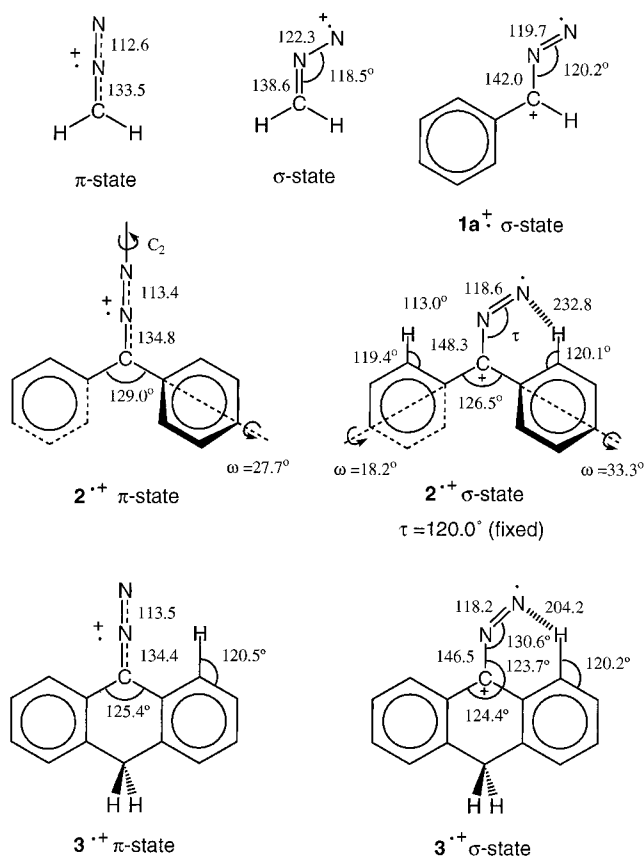
of the terminal nitrogen atom with the ortho hydrogen atom of the neighboring phenyl ring (cf. Figure 9). Such a distortion leads, of course, to an artificial destabilization of the σ-state, but this effect may be partly offset by the stabilization due to two coplanar phenyl rings.

Another estimate of the σ/π-energy gap in **2**[•+] was obtained by fixing the C−N−N angle in that compound at 120° (the value which prevails in σ-**1a**[•+]), whereby a σ-radical state was "enforced", and optimizing the rest of the molecule. Such a procedure resulted in the structure depicted in Figure 9, with an energy of 22.3 kcal/mol above that of the π-radical minimum. This (probably more realistic) value is higher than that in **3**[•+] because now the phenyl rings are no longer coplanar with the bent CN_2 group and are, therefore, less effective in stabilizing the σ- relative to the π-radical state (cf. Figure 1).

Although we cannot provide a definitive prediction of the σ/π-gap in **2**[•+], it becomes clear from the above results that it must be ≥20 kcal/mol in the isolated molecule. This conclusion is in marked contrast with the experimental findings which indicate that in condensed phase the two states are competitive in energy. Hence, solvent effects must be responsible for the change of the ordering of states from that which seems to prevail in the gas phase.

However, we are looking at a preferential solvation of the σ- over the π-radical state of ≥20 kcal/mol for **2**[•+] and **3**[•+], or up to 30 kcal/mol for **1a**[•+], which probably cannot be accounted for by continuum effects. Indeed, self-consistent reaction field (SCRF) calculations including a solvent with ϵ = 2.3 (corresponding to $CFCl_3$) revealed only minor effects of the solvent's electrostatic field on the σ/π-energy gap of **1a**[•+] (where the two states can be clearly distinguished without

interfering steric effects). Thus, we resorted to considering specific interactions between $1a^{•+}$ and the chlorine atoms of halogenated solvents, which could conceivably lead to chloronium-type cations, as they have been observed previously, for example, in the case of ester radical cations.[48−50]

A variety of possible complexes of one or two CH_3Cl or CH_2Cl_2 molecules with the σ- and π-radical states of $1a^{•+}$ were considered. However, no minima corresponding to chloronium-type cations could be located, mainly because such an interaction would have impaired the benzyl cation resonance which prevails in the σ-state of $1a^{•+}$ (where the positive charge is formally located on the diazo carbon atom, see section 5). The most stable forms of the complexes arose by interaction of the chlorine atoms with the slightly acidic hydrogen atom at the diazo group of $1a^{•+}$ and the terminal nitrogen atom of the σ-radical state but, even in this case, the preferential stabilization of the σ-radical state never amounted to more than a few kcal/mol. Furthermore, a C−N−N angle of 120° had to be enforced in all calculations in order to prevent spontaneous collapse into the much more stable π-state.

Although we have certainly not exhausted all possibilities of interaction between $1a^{•+}$ with the various solvents used in our study, it is safe to say that continuum electrostatic effects or conventional complexation with a molecule containing one or two chlorine atoms cannot be responsible for the observed reversal of the σ/π-energy difference on going from the gas phase to solution. If it were only for the solution studies, one might argue that the counterion and/or the presence of the ammoniumyl oxidant may be exercising a special effect, but in view of the results of the experiments with Freon matrices, where the counterions are not presumed to be in direct contact with the radical cations, such an explanation also seems unlikely. In these experiments, the mere change from $CFCl_3$ to the brominated Freon, CF_2BrCF_2Br, suffices to induce a crossover from the σ-radical to the π-radical state. Also, the optical spectra in glassy butyl chloride reported in 1987 by Kato et al.[5] pointed to the π-radical state of $2^{•+}$, a finding which indicates that there is nothing special about the Br-containing Freon.

5. Valence Structure of the σ-States of Diazomethane Radical Cations

Before concluding, we wish to point out an interesting feature which emerged from the calculations presented in Figure 9. The geometry of the diazo group in the linear π-state of the diazomethane radical cations[51] is nearly invariant to aryl substituion. In contrast, the bond lengths in the bent σ-state undergo significant changes in the course of such substitution. The C−N bond lengthens from 138.6 pm for the parent radical cation (similar to the C−N bond length in pyridine) via 142.0 pm for $1a^{•+}$ to 148.3 pm in $2^{•+}$ (similar to a C−N single bond in amines), while the N−N bond shortens concomitantly from 122.3 via 119.7 to 118.6 pm along the same series.

These geometry changes indicate a gradual changeover in the dominant valence structure from one where spin and charge reside in the $p_σ$-AO of the terminal nitrogen atom and which has a C═N double bond (cf. diazomethane in Figure 9) to one where the charge is formally located in the $p_π$-AO of the carbon atom and which has a N═N double bond (cf. the valence structure drawn for $1a^{•+}$). The reason for this changeover is, that the second valence structure becomes more stable by virtue of the resonance energy which is gained by placing the charge into the benzylic π-system of $1a^{•+}$ and, even more so, into the diphenylmethyl one of $2^{•+}$.[52] Thus, it is legitimate to write different valence structures for the σ-states of the radical cations of diazomethane and its aryl-substituted derivatives.

Conclusions

We have shown by optical and ESR spectroscopy that small changes in the solvent or in the conditions for oxidation can lead to a drastic change in the electronic and molecular structure of aryldiazo radical cations, from a linear allylic π- to a bent σ-radical state. Both states were observed in the radical cations of diphenyldiazomethane (**2**) and of 5-diazo-10,11-dihydro-5H-dibenzo[a,d]cycloheptene (**4**), whereas only the π-radical state could be formed in the radical cation of 9-diazo-9,10-dihydro-10,10-dimethylanthracene (**3**), in which the two phenyl rings are forced into a coplanar position with the $(C_{ipso})_2$−CN_2 plane. Table 2 summarized these findings.

In contrast to earlier suggestions by Ishiguro et al.,[1,2] quantum chemical calculations lead us to conclude that the observed small energy difference between the π-radical and the σ-radical state (σ/π-gap) of aryldiazo radical cations is by no means a property of the isolated molecules, but must be due to some specific solvent and/or counterion effects which were, however, not identified in the present study. In the isolated radical cations, the σ/π-gap is around 30 kcal/mol for that of phenyldiazomethane (**1a**) and 20 kcal/mol for that of diphenyldiazomethane (**2**). Thus, any attempt to explain the experimentally observed near-degeneracy of the two states must account for a preferential stabilization of the σ-radical state by an energy of this order of magnitude.

Supporting Information Available: Tables containing Cartesian coordinates and total energies corresponding to the B3LYP/6-31G*-optimized geometries of all compounds discussed in this study (ASCII). Table listing the experimental and calculated hyperfine data characterizing the σ- and π-structures of $2^{•+}$ and $4^{•+}$, as well as the π-structure of $3^{•+}$. Figures showing the ESR spectra of $2^{•+}$ and $[^{13}C]2^{•+}$ in Freon matrices, as well as the ESR spectrum of $3^{•+}$ and the ESR and ENDOR spectra of $6^{•+}$ generated electrolytically in dichloromethane (PDF). This material is available free of charge via the Internet at http://pubs.acs.org.

(48) Becker, D.; Plante, K.; Sevilla, M. D. *J. Phys. Chem.* **1983**, *87*, 1648.

(49) To validate the B3LYP method for this type of application, the binding energy of CH_3Cl with the ethyl cation ($\Delta H_{exp} = 30.7$ kcal/mol)[50] was calculated. This energy was found to be 33 kcal/mol (32.2 kcal/mol after correcting for the basis set superposition error), hence B3LYP is expected not to underestimate the binding energies of chloronium cations.

(50) Sharma, D. K. S.; deHöjer, S. M.; Kebarle, P. *J. Am. Chem. Soc.* **1985**, *107*, 3757.

(51) As the allylic π-MO is essentially nonbonding, the geometry of diazomethane undergoes only minor changes on ionization (with B3LYP/6-31G*, the C−N bond lengthens by 4 pm, the N−N bond shortens by 2 pm).

(52) This structural feature is also reflected in the Mulliken charge distribution: In the diazomethane radical cation, 18% of the positive charge is on the N_2 group, whereas in $2^{•+}$ the N_2 group bears a *negative* charge of 0.09 and the entire positive charge is in the CPh_2 moiety. Note that this marked change in the distribution of charge does not greatly affect that of the *spin*, because in both valence structures the unpaired spin resides formally in the $p_σ$-AO of the terminal nitrogen atom.